PHYSICAL REVIEW A **70**, 021601(R) (2004)

Measurement of the interaction strength in a Bose-Fermi mixture with ^{87}Rb and ^{40}K

J. Goldwin, S. Inouye, M. L. Olsen, B. Newman,* B. D. DePaola,† and D. S. Jin‡
JILA, National Institute of Standards and Technology, University of Colorado, Boulder, Colorado 80309, USA
(Received 5 May 2004; published 11 August 2004)

A quantum degenerate, dilute gas mixture of bosonic and fermionic atoms was produced using ^{87}Rb and ^{40}K. The onset of degeneracy was confirmed by observing the spatial distribution of the gases after time-of-flight expansion. Furthermore, the magnitude of the interspecies scattering length between the doubly spin-polarized states of ^{87}Rb and ^{40}K, $|a_{\mathrm{RbK}}|$, was determined from cross-dimensional thermal relaxation. The uncertainty in this collision measurement was greatly reduced by taking the ratio of interspecies and intraspecies relaxation rates, yielding $|a_{\mathrm{RbK}}|=250\pm30\ a_0$, which is a lower value than what was reported in [M. Modugno *et al.*, Phys. Rev. A **68**, 043626 (2003)]. Using the value for $|a_{\mathrm{RbK}}|$ reported here, current $T=0$ theory would predict a threshold for mechanical instability that is inconsistent with the experimentally observed onset for sudden loss of fermions in [G. Modugno *et al.*, Science **297**, 2240 (2002)].

DOI: 10.1103/PhysRevA.70.021601 PACS number(s): 03.75.Ss, 34.50.−s

With many recent advances, ultracold Fermi gas experiments are now beginning to explore the strongly interacting regime, where pairing can lead to fermionic superfluidity [1]. A natural extension to such studies is to investigate the properties of a mixture of a Fermi gas and a Bose-Einstein condensate (BEC). The presence of a BEC can vastly modify the static and dynamic character of a quantum degenerate Fermi gas. Mølmer pointed out that the mixture can phase separate, coexist, or collapse, depending on the relative sign and magnitude of the boson-boson and boson-fermion scattering lengths [2]. The spectrum of collective excitations can show rich physics as the interaction strength between the gases increases [3]. In addition, an effective fermion-fermion attraction arises from the boson-fermion interaction, which can significantly increase T_c for a phase transition to a BCS-type superfluid [4]. This mechanism for the Cooper pairing of atoms is intriguing because of the analogy to superconductivity.

To date, quantum degenerate atomic Bose-Fermi mixtures have been realized in the following combinations: ^{6}Li (fermion) with ^{7}Li (boson) [5], ^{6}Li with ^{23}Na (boson) [6], and ^{40}K (fermion) with ^{87}Rb (boson) [7]. With the last mixture, pioneering experiments by the LENS group revealed that the scattering length between ^{87}Rb and ^{40}K is large and negative [7–10]. At high densities, this strong attractive interaction can exceed the Pauli pressure and cause the whole system to become mechanically unstable and collapse [2,10–13]. The LENS group has reported the observation of such a collapse; they see a sudden loss of ^{40}K atoms as the number of atoms in the ^{87}Rb BEC exceeds a threshold value [8].

Here we report the production of a quantum degenerate Bose-Fermi mixture with ^{87}Rb and ^{40}K atoms and a determination of the magnitude of the cross-species scattering length. Our experimental apparatus for producing the mixture, which requires only a single magneto-optical trap (MOT), is outlined in Fig. 1. In brief, our vacuum chamber consists of two glass cells—one contains a two-species MOT while the other cell (science cell) is used for evaporative cooling of the mixture. The lifetime for ^{87}Rb atoms in the magnetic trap, which is limited by collisions with the background gas, is ~4 s in the MOT cell and more than 100 s in the science cell. The atoms are transferred between the cells using a moving magnetic trap.

The experimental procedure for creating the mixture is as follows. First, 2×10^{9} ^{87}Rb atoms and 1×10^{7} ^{40}K atoms are collected in a two-species MOT from the background vapor [14]. The atoms are then transferred into a quadrupole magnetic trap, whose magnetic field gradient along the symmetry axis in the horizontal direction is 99 G/cm. During the last 50 ms of the MOT, the ^{87}Rb cloud is compressed by reducing the intensity of the hyperfine repumping light. Simultaneously the ^{40}K cloud is Doppler cooled by reducing the detuning of the trapping light to about one natural linewidth (~6 MHz). In addition, the atoms are optically pumped to

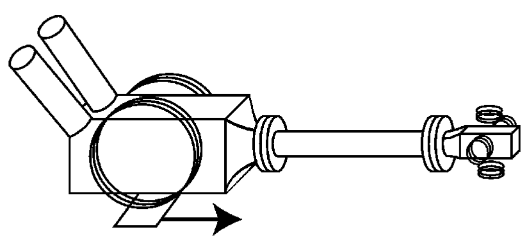

FIG. 1. Schematic of the experimental apparatus. The glass cell on the left ("MOT cell") is filled with a background vapor of ^{87}Rb and ^{40}K released from alkali-metal dispensers attached to the left end of the cell. The cell on the right ("science cell") is under ultrahigh vacuum, and small coils surrounding the cell produce a magnetic trap with strong confinement for evaporative cooling. (The figure does not show all the coils.) Atoms are transferred from the MOT cell to the science cell using a moving magnetic trap produced by an anti-Helmholz coil pair on a translation stage.

*Present address: Department of Physics, MIT, Cambridge, MA 02139, USA.

†Permanent address: J. R. Macdonald Laboratory, Department of Physics, Kansas State University, Manhattan, KS 66506, USA.

‡Quantum Physics Division, National Institute of Standards and Technology.

their doubly spin-polarized states, which are $|F,m_F\rangle=|2,2\rangle$ for ^{87}Rb and $|9/2,9/2\rangle$ for ^{40}K. Once in the quadrupole magnetic trap, the atoms are transferred to the science cell by physically moving the trapping coils, which are mounted on a motorized translation stage [15]. The observed loss in the phase-space density of the ^{87}Rb cloud during the 81 cm (6 s) travel is only a factor of 2. In the science cell, the atoms are transferred to an Ioffe-Pritchard-type magnetic trap for the final cooling. Since there is no MOT in the science cell, the cell size can be small (our cell is 1 cm^2 in the cross section) and we can place coils very close to the atoms to achieve tight confinement with relatively low electric current ($\sim$27 A). The radial (axial) trapping frequency for ^{87}Rb is $\nu_{r,\mathrm{Rb}}=160$ Hz ($\nu_{r,\mathrm{Rb}}=25$ Hz), and the trapping frequencies for ^{40}K are $\sqrt{m_{\mathrm{Rb}}/m_{\mathrm{K}}}=1.47$ times higher, where m_{Rb} (m_K) is the mass of ^{87}Rb (^{40}K) atoms.

Simultaneous quantum degeneracy is achieved by radio frequency (rf)-induced evaporative cooling of ^{87}Rb and sympathetic cooling of ^{40}K. This scheme circumvents the problem of vanishing elastic cross section for spin-polarized fermions at ultracold temperatures [16]. The typical initial number and temperature of the ^{87}Rb atoms in the Ioffe-Prichard trap before evaporation are $N_{\mathrm{Rb}}=3\times10^8$ and $T_{\mathrm{Rb}}=400\ \mu$K; with these initial conditions, we produce a nearly pure BEC of 2×10^5 ^{87}Rb atoms after 40 s of evaporation. The initial conditions for ^{40}K in the Ioffe-Prichard trap are not known due to the difficulty of measuring a small optical density cloud with absorption imaging. For sympathetic cooling from 10 to 0.4 μK, a range where the ^{40}K cloud can be imaged and there is not yet a ^{87}Rb BEC, we observe less than 10% number loss with typically 1.4×10^5 ^{40}K atoms.

Quantum degeneracy for the ^{87}Rb gas is evident in the formation of a Bose-Einstein condensate, which is characterized by the emergence of a bimodal distribution in the absorption images taken after time-of-flight expansion. The fraction of atoms in the BEC is determined by fitting the distribution with the sum of the Thomas-Fermi profile (inverted parabola) for the condensate and the thermal distribution for an ideal Bose gas [Fig. 2(a)]. The temperature is determined from the fit to the noncondensed component. For comparison to our data, a theory curve that includes both the effects from finite number and the positive chemical potential due to boson-boson interactions in the condensate is also shown [17]. The theory and the experiment are in good agreement. These data were taken with $\sim1\times10^4$ ^{40}K atoms present at the end of evaporation. In comparing data taken with and without ^{40}K atoms present, no effect of ^{40}K on the ^{87}Rb condensate fraction is observed. This is consistent with the low ^{40}K density ($\sim3\times10^{12}$ cm^{-3}), which results in a negligible contribution to the ^{87}Rb mean field.

The effect of quantum degeneracy on fermions is more subtle. The density distribution in time of flight becomes more "flat topped" than that for a classical gas due to the Pauli pressure. The fugacity $z=\exp(\mu_K/k_BT)$ (where μ_{K} is the chemical potential of ^{40}K), the cloud size in each direction, and the peak density of the gas are used as independent parameters for fitting the images. In Fig. 2(b) the measured fugacity is plotted as a function of T/T_F, where T is determined from the cloud size, and T_F is the Fermi temperature.

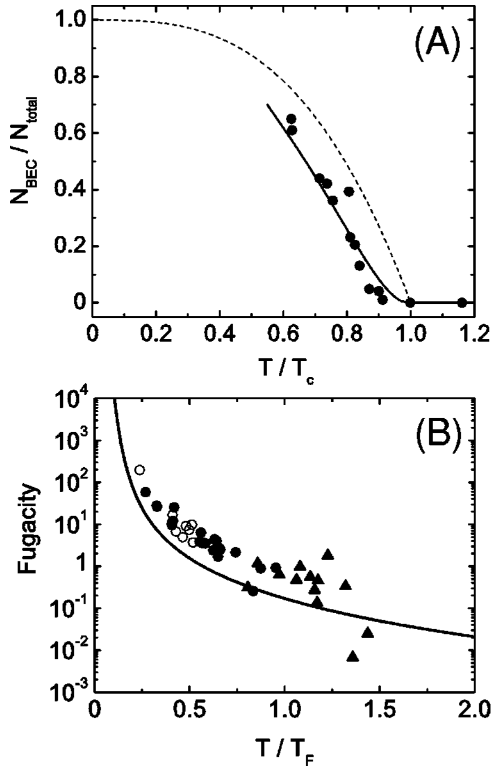

FIG. 2. Quantum degeneracy observed in time-of-flight images. (a) Condensate fraction $N_{\mathrm{BEC}}/N_{\mathrm{total}}$ obtained from 20 ms time-of-flight images of ^{87}Rb. The dashed line shows the condensate fraction for an ideal Bose gas in the thermodynamic limit. The solid line includes the effects from the finite number of atoms and the positive chemical potential due to boson-boson interactions in the condensate [17]. The phase transition occurs at 440 nK. (b) Fugacity of the fermionic cloud obtained by fitting the density distribution of ^{40}K atoms after 5 ms time of flight. The fugacity z is equal to the peak phase space density of the gas in the classical limit. The different symbols denote data taken with a ^{87}Rb BEC present (filled circles), with a ^{87}Rb thermal cloud present (filled triangles), and without ^{87}Rb atoms present (open circles). The data are systematically shifted from the theory curve expected for an ideal Fermi gas (line). A typical value of T_F at $T/T_F=0.5$ is 220 ± 50 nK.

From the fugacity, measurement, and assuming an ideal Fermi gas, we find that the lowest T/T_F achieved in this experiment was 0.2. For comparison to the data, the solid line shows the prediction for an ideal Fermi gas in a three-dimensional harmonic trap [18]. Most of the data lie to the right of the curve. This discrepancy could be explained if our ^{40}K number calibration is low by about a factor of 2 so that T/T_F is systematically overestimated by 20%. Note that the fugacity, which is a measure of the "flatness," is free from calibration errors. The temperature measurement has been confirmed by fitting to the thermal wing of ^{87}Rb images taken during the same experimental run. Finally, we note that the measured fugacity shows no systematic difference between ^{40}K images taken with and without a ^{87}Rb BEC present in the trap. With our highest number of 1.8×10^5 ^{87}Rb atoms in a BEC and 8×10^4 ^{40}K atoms in the Fermi gas we observe only a slow number loss ($\sim$1 s time scale) and no sudden collapse.

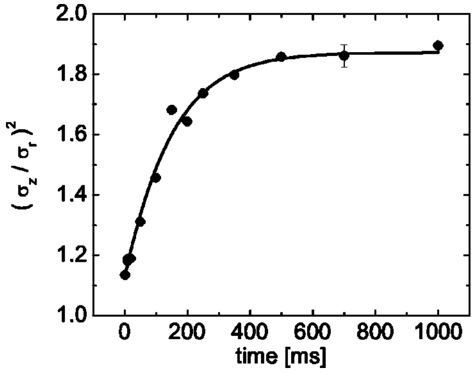

FIG. 3. Typical relaxation curve for the energy anisotropy. Shown is the square of the ^{40}K cloud aspect ratio after 5 ms time of flight; this is proportional to the ratio of the energies in each direction. The ^{40}K cloud rethermalizes through elastic collisions with ^{87}Rb atoms. The line is a fit to the ratio of exponentially decaying curves. The error bar represents only the statistical uncertainty.

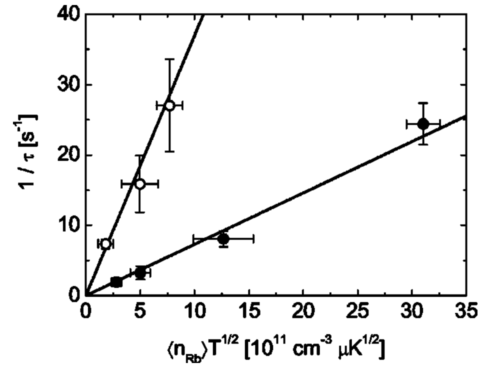

FIG. 4. Measurement of the elastic collision cross section through energy anisotropy relaxation. Relaxation time constants for a ^{40}K gas in the presence of ^{87}Rb (open circles) and ^{87}Rb gas alone (filled circles) are shown as a function of the product of average ^{87}Rb density in the trap and the square root of the equilibrium temperature. Lines are linear fits through the origin. The ratio of the slopes is used to extract the magnitude of interspecies scattering length $|a_{\mathrm{RbK}}|$, as shown in Eq. (3).

The strength of interspecies interactions is critical in determining the static and dynamic properties of the mixture. We have determined the magnitude of the interspecies scattering length $|a_{\mathrm{RbK}}|$ through measurements of cross-dimensional thermal relaxation [19]. In general, this method has limited accuracy because of systematic uncertainties in the atom number, which is typically determined from absorption imaging. Experimental imperfections such as frequency jitter, imperfect polarization of the probe beam, or fluctuation and tilt of the magnetic field during imaging tend to reduce probe beam absorption. This leads to an underestimate of the number of atoms and an overestimate of the cross-section. Here we avoid this systematic error by taking the ratio of two cross-section measurements that are both proportional to the number of ^{87}Rb atoms: (1) thermal relaxation of ^{40}K atoms in the presence of ^{87}Rb and (2) relaxation of a single-species ^{87}Rb cloud. We further use the fact that the Rb-Rb cross section is already known with high accuracy [20].

The experimental procedure is as follows. First, we prepare 1×10^5 ^{40}K atoms and 4×10^5 ^{87}Rb atoms at temperatures $T\sim 1$ μK in a magnetic trap whose radial trapping frequency $\nu_{r,\mathrm{Rb}}$ is 90 Hz. Both gases are away from quantum degeneracy and elastic collisions are in the *s*-wave limit. Multiple 1 ms rf sweeps can be applied to reduce the number of ^{87}Rb atoms by as much as a factor of 4, for the purpose of varying the density. The bias magnetic field is then ramped from 4.3 to 1.4 G to increase the radial confinement of the magnetic trap to its regular strength ($\nu_{r,\mathrm{Rb}}=160$ Hz); this adds energy to the radial direction. The duration of the ramp is kept long ($\geqslant$10 ms) compared to the radial trapping period to avoid excitation of collective modes, but short compared to the relaxation time in the gas. This is always possible unless the gases enter into the hydrodynamic regime.

Just after the ramp, the energy of the gas in the radial direction is higher than in the axial direction. The cross-dimensional rethermalization time constant is extracted by holding the mixture for a variable time in the final trap and measuring the aspect ratio after time of flight. Shown in Fig. 3 is a typical relaxation curve for the energy anisotropy. Rather than the radial and axial sizes, the aspect ratio of the cloud, σ_z/σ_r, is used for data analysis since it is less sensitive to shot-to-shot variations in the absolute temperature of the cloud before the compression [21].

The data analysis is simplified by two facts: (i) due to the Fermi statistics, the spin-polarized ^{40}K atoms collide only with ^{87}Rb atoms, and (ii) in our experiment there is no net flow of energy between the ^{40}K and ^{87}Rb gases. Therefore, the thermal relaxation rate of the ^{40}K cloud, $1/\tau_{\mathrm{K}}$, depends only on the collision rate with ^{87}Rb atoms [22]:

$$\frac{1}{\tau_{\mathrm{K}}} = \frac{1}{\beta}\langle n_{Rb}\rangle\ \sigma_{\mathrm{RbK}}\ v_{\mathrm{RbK}}. \tag{1}$$

Here, $\langle n_{Rb}\rangle$ is the average density of ^{87}Rb atoms in the trap, $\sigma_{\mathrm{RbK}}=4\pi a_{\mathrm{RbK}}^2$ is the elastic cross section for Rb-K collisions, and $v_{\mathrm{RbK}}=\sqrt{8k_BT/\pi\mu}$ is the thermally averaged relative speed between ^{87}Rb and ^{40}K atoms, where $\mu = m_{\mathrm{Rb}}m_{\mathrm{K}}/(m_{\mathrm{Rb}}+m_{\mathrm{K}})$ is the reduced mass. The coefficient of proportionality, β, can be regarded as the number of collisions per ^{40}K atom needed for thermal relaxation. The relaxation rate for a single-species ^{87}Rb cloud $1/\tau_{\mathrm{Rb}}$ is proportional to the Rb-Rb collision rate

$$\frac{1}{\tau_{\mathrm{Rb}}} = \frac{1}{\alpha}\langle n_{Rb}\rangle\ \sigma_{\mathrm{RbRb}}\ v_{\mathrm{Rb}}, \tag{2}$$

where $\sigma_{\mathrm{RbRb}}=8\pi a_{\mathrm{Rb}}^2$ is the elastic cross section for Rb-Rb collisions, $v_{\mathrm{Rb}}=4\sqrt{k_BT/\pi m_{\mathrm{Rb}}}$ is the thermally averaged relative speed between ^{87}Rb atoms, and α is the coefficient of proportionality for single-species relaxation. Thus, the ratio of the two time constants is free from systematic uncertainties in the ^{87}Rb number [23].

$$\frac{\tau_{\mathrm{Rb}}}{\tau_{\mathrm{K}}} = \frac{1}{2}\frac{\alpha}{\beta}\sqrt{\frac{m_{\mathrm{Rb}}}{2\mu}}\left(\frac{a_{\mathrm{RbK}}}{a_{\mathrm{Rb}}}\right)^2. \tag{3}$$

The constant α (β) has been determined to be 2.67 ± 0.13 (2.1 ± 0.2) from Monte Carlo simulations using our experimental parameters, including the initial energy anisotropy of both species and the mass difference between ^{40}K and ^{87}Rb [24]. It is this mass difference that gives rise to the difference between α and β, as a lighter particle can redistribute more of its total kinetic energy in a single collision.

The measured relaxation rates for varying densities of ^{87}Rb atoms are plotted in Fig. 4. The error bars only account for statistical errors. Systematic uncertainties in the ^{87}Rb density were eliminated from the determination of $|a_{\mathrm{RbK}}|$ by taking the ratio of the two slopes and using Eq. (3). The known value $a_{\mathrm{Rb}}=98.98\pm0.04\ a_0$ for ^{87}Rb in the $|2,2\rangle$ state [20], obtained by combining multiple high-precision measurements including photoassociation and Feshbach spectroscopy, is used for calibration [25] and we obtain $|a_{\mathrm{RbK}}| = 250\pm30\ a_0$.

This measured value of $|a_{\mathrm{RbK}}|$ is in mild disagreement with the value of $-410^{+80}_{-90}\ a_0$ from the LENS group [8], which was determined from a collisional measurement that had the usual large systematic number uncertainty. More serious disagreement is seen when comparing our result with the value of $-395\pm15\ a_0$ determined from a comparison of theory predictions and experimental observation of collapse phenomena [10]. These results suggest a need for further investigation of the behavior of the mixture close to the collapse. For example, the zero-temperature phase diagram in Ref. [12] which assumed $a_{\mathrm{RbK}}=-260\ a_0$ predicts that a condensate with 2×10^6 atoms remains mechanically stable with numbers of ^{40}K atoms as high as 1×10^7. The new value for $|a_{\mathrm{RbK}}|$ that we report here is also likely to have an impact on the predicted positions of Feshbach resonances [26,27].

The authors thank Eric Cornell and Carl Wieman for useful discussions. We acknowledge support from the U.S. Department of Energy, Office of Basic Energy Sciences, the W. M. Keck Foundation, and the National Science Foundation. B.D.D. expresses his thanks to the JILA Visiting Fellow program.

[1] See, for example, C. A. Regal, M. Greiner, and D. S. Jin, Phys. Rev. Lett. **92**, 040403 (2004).
[2] K. Mølmer, Phys. Rev. Lett. **80**, 1804 (1998).
[3] S. K. Yip, Phys. Rev. A **64**, 023609 (2001); T. Miyakawa, T. Suzuki, and H. Yabu, Phys. Rev. A **62**, 063613 (2000); T. Sogo *et al.*, *ibid.* **66**, 013618 (2002); P. Capuzzi, A. Minguzzi, and M. P. Tosi, *ibid.* **68**, 033605 (2003); X-J. Liu and H. Hu, *ibid.* **68**, 033613 (2003).
[4] M. J. Bijlsma, B. A. Heringa, and H. T.C. Stoof, Phys. Rev. A **61**, 053601 (2000); H. Heiselberg *et al.*, Phys. Rev. Lett. **85**, 2418 (2000); L. Viverit, C. J. Pethick, and H. Smith, Phys. Rev. A **61**, 053605 (2000); L. Viverit, *ibid.* **66**, 023605 (2002).
[5] A. G. Truscott *et al.*, Science **291**, 2570 (2001); F. Schreck *et al.*, Phys. Rev. Lett. **87**, 080403 (2001).
[6] Z. Hadzibabic *et al.*, Phys. Rev. Lett. **88**, 160401 (2002).
[7] G. Roati *et al.*, Phys. Rev. Lett. **89**, 150403 (2002).
[8] G. Modugno *et al.*, Science **297**, 2240 (2002).
[9] G. Ferrari *et al.*, Phys. Rev. Lett. **89**, 053202 (2002); F. Ferlaino *et al.*, J. Opt. B: Quantum Semiclassical Opt. **5**, S3 (2003).
[10] M. Modugno *et al.*, Phys. Rev. A **68**, 043626 (2003).
[11] R. Roth and H. Feldmeier, Phys. Rev. A **65**, 021603 (2002).
[12] R. Roth, Phys. Rev. A **66**, 013614 (2002).
[13] T. Miyakawa, T. Suzuki, and H. Yabu, Phys. Rev. A **64**, 033611 (2001); X.-J. Liu, M. Modugno, and H. Hu, *ibid.* **68**, 053605 (2003); A. P. Albus, F. Illuminati, and M. Wilkens, *ibid.* **67**, 063606 (2003).
[14] J. Goldwin *et al.*, Phys. Rev. A **65**, 021402 (2002).
[15] H. J. Lewandowski *et al.*, J. Low Temp. Phys. **132**, 309 (2003); H. J. Lewandowski, Ph.D. thesis (2002); (http://jilawww.colorado.edu/www/sro/thesis/).
[16] B. DeMarco *et al.*, Phys. Rev. Lett. **82**, 4208 (1999).
[17] M. Naraschewski and D. M. Stamper-Kurn, Phys. Rev. A **58**, 2423 (1998).
[18] D. A. Butts and D. S. Rokhsar, Phys. Rev. A **55**, 4346 (1997).
[19] C. Monroe *et al.*, Phys. Rev. Lett. **70**, 414 (1993).
[20] E. G.M. van Kempen *et al.*, Phys. Rev. Lett. **88**, 093201 (2002).
[21] The measured equilibrium aspect ratio is higher than that for an isotropic energy distribution with purely ballistic expansion. We attribute this to imperfections in the trap turnoff, and include a 10% uncertainty in T in our error bar for $|a_{\mathrm{RbK}}|$.
[22] This equation is equivalent to Eq. 1 in I. Bloch *et al.*, Phys. Rev. A **64**, 021402 (2001), with a zero intraspecies cross section.
[23] Note that the average density of ^{87}Rb ($\langle n_{\mathrm{Rb}}\rangle$) in Eq. (1) is taken over the ^{40}K density distribution, while that in Eq. (2) is taken over the ^{87}Rb distribution. These differ only by a temperature-dependent factor due to the different equilibrium positions of the clouds due to gravity. For these data this effect is limited to 3 to 5%, and is included in the analysis.
[24] J. Goldwin *et al.*, in preparation.
[25] Equation (2) with single-species data in Fig. 4 yields $a_{\mathrm{Rb}} = 109\ a_0$, which is 10% larger than the accepted scattering length of ^{87}Rb in the $|F,m_F\rangle=|2,2\rangle$ states. This corresponds to a 20% underestimation of our ^{87}Rb number.
[26] A. Simoni *et al.*, Phys. Rev. Lett. **90**, 163202 (2003).
[27] Recently we have observed multiple interspecies Feshbach resonances: S. Inouye *et al.*, e-print cond-mat/0406208 (2004).